

OIL SPILL DETECTION IN SAR SATELLITE IMAGES: A REVIEW

IRINA GANCHEVA

Department of Meteorology and Geophysics

Ирина Ганчева. РАЗПОЗНАВАНЕ НА НЕФТЕНИ РАЗЛИВИ НА SAR-СПЪТНИКОВИ ИЗОБРАЖЕНИЯ: ОБЗОРНА СТАТИЯ

Акцентът на тази обзорна статия е преглед на различни техники за автоматично откриване на нефтени разливи посредством анализ на SAR-(радар със синтетична апертура) спътникови изображения. Разглежда се физическото поведение на нефт върху водна повърхност и неговият ефект върху отразения или излъчения сигнал, като се представят и различни методи за широкомащабно наблюдение на океана. Обърнато е внимание на възможностите за оперативно внедряване. SAR-сензорите са разгледани подробно. Обобщени са последователните стъпки в разработването на автоматичен алгоритъм за откриване на нефтени разливи.

Irina Gancheva. OIL SPILL DETECTION IN SAR SATELLITE IMAGES: A REVIEW

This article examines different techniques for automatic detection of oil spills using Synthetic Aperture Radar satellite images. The physical behavior of oil on water surface and its effect on the reflected or emitted signal is reviewed and different methods for large scale oil spill ocean monitoring are presented, discussing in particular their operational use. The SAR sensors are reviewed in details. The different steps in the development of an automatic algorithm for the detection of oil slick are described in details.

Keywords: oil spill, automatic algorithms, SAR satellite images

PACS numbers: 92.20 Ny, 92.20 Wx

For contact: Irina Gancheva, Department of Meteorology and Geophysics, Faculty of Physics, Sofia University “St. Kliment Ohridski”, 5 James Bourchier Blvd., Sofia 1164, Bulgaria, Phone: +359 2 8161289, E-mail: irina.gancheva@phys.uni-sofia.bg

1. INTRODUCTION

The environmental hazard of oil for the marine system has been studied and known for long time [1] and still oil spills are observed relatively often due to accidental or deliberate oil discharges. Some of the big oil pollution accidents such as the Deepwater Horizon spill in the Gulf of Mexico in 2010 or the Prestige tanker near the coast of Galicia in 2002 have attracted significant media interest and social outrage. Even though according to ESA accidental discharges hold only 7% of the oil pollution and operational discharges from tankers in rivers and oceans sum up to 80% of the oil spills [2]. Unfortunately in most cases they remain not traced.

There are various methods for ocean surface monitoring however the spaceborne remote sensing has proven to be one of the most efficient because of the large range of provided spectral information, great accuracy and high frequency of provided data. The identification of an oil spill, its extent and the type of the spill – if crude or natural oil – can be gained by this type of monitoring. The combination of this information with airborne monitoring can provide additional evidences about the pollutant. Very often it is necessary to analyse data from different sensors and wavelengths in order to discriminate between alga blooms, look-alikes and man-made slicks. The calculation of a set of features, such as contrast, shape, homogeneity and slick surroundings can contribute with additional clues for the detected object and thus support to distinguish actual oil from look-alikes. These procedures could significantly reduce the false alarm ratio for the automatic oil spill detection.

Synthetic Aperture Radar (SAR) compared to other methods remains the most efficient satellite sensor for oil spill detection exploring large areas regardless daytime and weather conditions. These type sensors provide regularly data and can detect even small amounts of oil without the need for good image resolution. The satellites equipped with SAR deliver data from different frequency bands, making it useful for various environmental purposes. This method presents also some limitations: it does not deliver information for the oil thickness and type. Some problems appear also due to the wind and water interaction.

Other space- and airborne methods for oil spill detection include visual, infrared and ultraviolet remote sensing, laser fluorosensors, microwave radiometers and scatterometers. All of them are useful and partly advantageous compared to SAR, however so far they have had only limited success for accurate, regular and spacious ocean monitoring.

Some good reviews on oil slick detection making use of different monitoring methods have been already published. Fingas and Brown [3] have done an excessive study on the different methods for detection of oil and on discussing their advantages and disadvantages. Another major focus in their review is the description of the techniques for slick thickness measurements and for detection of oil in the whole water column and on the sea bottom.

Solberg's review [4] is a very valuable read with a main focus on SAR and space borne-based detection methods, discussing also manual and automatic detection approaches.

Alpers et al. [5] reviews the behaviour of different oil types on sea surface and presents some discrimination methods such as statistical approaches, using differences in the dielectric constant and polarimetric parameters.

Topouzelis [6] presents a study on oil slick monitoring using SAR images with a focus on the semi- and fully automatic methodologies for their detection. A special advantage of this review is the comparison between different dark object classification methods and their operational advantages and disadvantages.

Gens' review [7] covers different applications of SAR images for oceanographic purposes such as ocean wave imaging, ocean currents, sea-floor topography, oil spill and ship detection, wind speed, rainfall and others.

2. PHYSICAL BACKGROUND

There are different methods for oil spill monitoring depending on the sensor type being used. In order to estimate their theoretical feasibility the optical properties of oil and water should be considered first.

Measurements of the oil/water reflectivity and relative absorbance for different wavelengths have been done, however not across the whole spectrum and with limited accuracy [8–11]. In the review of Fingas and Brown [3] is presented a generalized summary of different measurements, coming to the conclusion that the oil/water reflectivity and relative absorbance have very similar behaviour for different wavelengths ranging from 200 to 1100 nm. The similarity in the properties of both media leads to the conclusion that considering only the visible spectrum would not be sufficient to firmly distinguish oil.

The visible remote sensing uses radiation with wavelength of 400–700nm and in this range oil has slightly higher surface reflectance than water. Nevertheless the absorption/reflection differences are rather small and usually not sufficient to clearly distinguish oil from water [12]. The use of polarized lenses has the potential of enhancing the visibility of oil and some authors investigate this effect [13], however a major difficulty for the visible remote sensing remains the issue to reduce the sun glitter, which might be confused for oil sheens [14, 15].

The biggest limitation for the visible remote sensing is the need for clear skies during the overpass, which is rarely the case. For the implementation of oil spill detection algorithms long time series of data are to be analysed, which is hard to be obtained considering the overpass period and the problems with the collection of usable data.

The use of infrared signal for the detection of oil slicks relies on the thermal properties of oil. It heats up faster than water and thick oil films absorb the solar radiation. Afterwards a portion is re-emitted as thermal energy and can

be distinguished from water by its higher temperature. Thus thick oil films will appear hot, those with intermediate thickness are cool and thin films cannot be detected by this method. Some studies have investigated the effect of thickness on the temperature and conclude that the minimum detectable layer is between 10 and 70 μm [3]. The exact reason why intermediate layers appear as cool is not completely understood, however the authors make a hypothesis about the destructive interference of thermal radiation waves.

An important limitation of the infrared detection technique is the fact that the longer oil stays on sea surface, the more it mixes with it and in general the emulsion cannot be detected with infrared sensors [16]. The reason is that the thermal conductivity of the emulsion is quite similar to the one of the ambient. It should be also mentioned that infrared scanning at night-time presents lower contrast of the images compared to daytime results [17], thus the operational use of that method is difficult. In addition, the sediments, seaweeds or other organic matter, shoreline and oceanic fronts interfere with the infrared signal. In conclusion, there are several major disadvantages of the infrared remote sensing for oil spill monitoring, which make it an unfavourable choice for the operational use.

Another technique for oil spill detection is analysing the images in the ultraviolet spectral band. In this range of the electromagnetic spectrum oil is highly reflective even for layers thinner than 0.1 μm . Earlier studies combine ultraviolet and infrared images to produce relative thickness map of oil slicks. However, ultraviolet signals are also affected by sun glints, biogenic material or wind slicks [18], which is a major limitation. This method is not widely used today due to the unimportance of the oil thickness when taking counteractions.

Another recent technique makes profit of laser fluorosensors. It is based on the excitation of some electronic states in the aromatic compounds in petroleum oils after absorption of ultraviolet light. These states release energy through fluorescence emission in the visible spectrum range [19–21]. The emitted radiation is of specific wavelength and can distinguish oil from other biologically active materials. Another benefit is that the detected signal provides information about the oil types. On the other hand, the major limitation is that this type of sampling is done with aircrafts and thus is rather inconvenient for large ocean areas.

Using microwave radiation for ocean monitoring can be done in two ways – with active and passive microwave sensors. For the purpose of oil spill detection the active remote sensing has proven to be more effective, as the passive sensing is dependent on weather conditions and daytime.

The passive microwave sensor measures the reflected space radiation, detecting the difference in the emissivity factor for water (0.4) and for oil (0.8) [22].



Fig. 1. A SAR image from Baltic sea. The dark objects marked with the white arrows are oil spills and the other dark formations are look-alikes; image from [4]

Additionally, the change of the signal with the oil film thickness provides a tool for measuring the spill thickness. A serious disadvantage is the unsatisfying spatial resolution, in the range of tens of meters for a radiometer. Some extensive studies on the usage of passive microwave sensors have been presented in [23–25].

The remote sensing in the microwave spectrum range in active mode is well studied and widely spread method, providing good results. The active microwave sensor, better known as radar, is widely used for ocean and land monitoring. It sends signals in the microwave range and by the detection of their reflectance amplitude and phase, one can examine the objects or landscape on the way. The resulting radar image of ocean surface is known as sea clutter, because the capillary waves reflect the incident radar signal and produce a bright image. On the other hand oil on the sea surface dampens the capillary waves and an oil slick appears as a dark area in the bright ocean [26]. Similar effect of damping the waves and receiving a dark spot on the ocean surface is gained by fresh water and wind slicks, glacial flour, biogenic oils and sea weeds, calming the water above them [7]. Extensive studies and classification of these and other look-alikes have been accomplished,

considering that they are the key for the dislocation of oil spills and false alarms. Still the percentage of false detected dark spots is around 20% [27].

Fig. 1 is an example of how oil spills and look-alikes are visible on a satellite images and it is a SAR image from the Baltic sea. The dark objects indicated with white arrows are actual oil spills and the other dark formations correspond to look-alikes. With this the challenges for the correct classification become obvious.

An important advantage of the active remote sensing technique is its implementation regardless weather conditions and daytime since its operation is not based on visible light and the water molecules in the air do not reflect the signal.

Radars used for military purposes are not useful for oil spill detection as they remove the clutter signal, essential for oil monitoring. The radars, which deliver the best information for environmental remote sensing, are Synthetic Aperture Radar (SAR) and Side-Looking Airborne Radar (SLAR). The images, produced by SAR are with a better resolution and greater range, making it the better option for ocean monitoring. An extensive comparison between SAR and SLAR is done by [28].

SAR radars send signals at different wavelengths, making them useful for various purposes. The frequency and the polarization of the SAR sensor have a significant impact on the detectability of oil slicks. The different SAR bands correspond to the wavelength of the transmitted signal – X-band (2.4 – 3.75cm), C-band (3.75–7.5cm), S-band (7.5–15cm), L-band (15–30cm) and P-band (30–100cm).

The accurate measurement of the surface roughness is the key for detecting anomaly patterns on sea surface with SAR. An adequate choice for the wavelength of the transmitted signal λ_i is essential, because the backscattered signal will be modified by the surface roughness at the same scale as λ_i . Kim et al. [29] has examined the expected dampening of the return signal as a function of the wavelength and showed that the dampening ratio of the X-band is higher than that of the C-band for fixed incidence angle and wind speed. The high ratio between the transmitted and the dampened signal is an indication for the presence of oil. For oil spill detection different studies have shown that the X-band delivers best results, followed by C-band and L-band [29–31], as the first two have approximately the same scale as the Bragg waves. For large incidence angles $\theta = 20^\circ - 60^\circ$ the scattering mechanism at the ocean surface can be described with the Bragg scattering theory due to the wavelength of the capillary waves which is about a couple of centimetres [32]. Using the L-band has proven to be the most inefficient one as the Bragg waves don't resonate with the incident signal causing much smaller dampening of the backscattered wave [33].

The polarization of the SAR signal plays an important role as well. There are horizontal (H) and vertical (V) polarization and the possible combinations of transmitted and received signal are HH, HV, VV and VH. There are studies analysing the quality and usability of the different polarization combinations [4, 34, 35]. For airborne radars the VV polarization provides the best results, however all combinations are reasonable to use. The HH polarization is suitable for ship detection, meaning that

combined observations usually deliver better results. In the last decade research on polarimetric SAR data has proven to deliver good results for oil spill detection [4, 36, 37]. In this case the polarimetric SAR sensor collects data of all combinations – co-polarized (VV and HH) and cross-polarized (VH and HV).

3. SATELLITES

The Synthetic Aperture Radar (SAR) is an active method for Earth observation and topography monitoring and more specifically their variations in time. A high resolution image of the examined surface can be obtained by analysing the intensity and phase of the received signal compared to the transmitted signal, as long as the scanned objects remain stationary over the scanning period of time. Alternatively the principle of SAR functioning can be explained by considering the Doppler shift of the echo signal. The vertical position of the objects can be determined comparing the upshift and downshift of the echo signal.

Tremendous reviews with information about the construction principles and function of SAR are presented in [38, 39].

For the in-depth understanding of SAR some geometrical definitions should be considered, as presented in figure 2. The SAR antenna is moving parallel to the Earth surface and vertical to the radar beam and its exact position is known at any time. The along track direction of the antenna is referred as azimuth or cross range and the perpendicular one – range or cross track. The footprint is the land piece scanned at the present moment and the swath is the land strip along which the antenna is moving. The swath width can vary from few kilometres up to 20 km for an airborne SAR and from 30 to 500 km for a spaceborne SAR.

The azimuth resolution δ_a of a SAR is given by the construction specification of the synthetic aperture or the path length during the echo signals from the target is received by the radar. It can be calculated using

$$\delta_a = r_0 \Theta_a = r_0 \frac{\lambda}{2L_{SA}} = \frac{d_a}{2}$$

with the factor two in the denominator because of the two-way path of the signal, r_0 – the slant range distance, $\Theta_a = \lambda/d_a$ – the virtual beam width, λ the radar signal-wavelength, L_{SA} – the synthetic aperture length and d_a – the antenna's length [38].

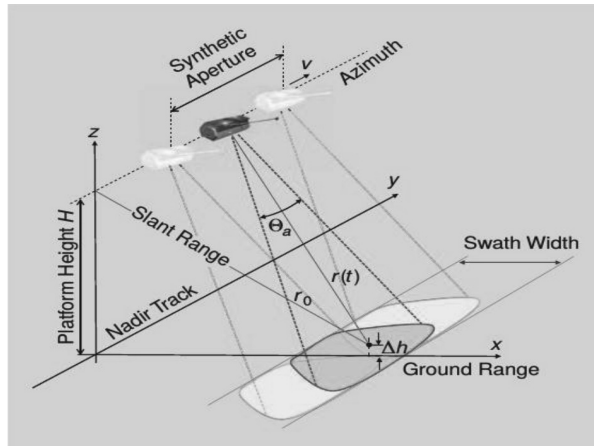


Fig.2. SAR geometry with illustration of some of the basic SAR terms; r_0 is the slant range, Θ_a – the azimuth beam width, and v is the sensor velocity; from [39]

The first approaches for ocean monitoring for oil spills emerged with the data, delivered by ERS, ENVISAT ASAR and RADARSAT-1. Later the launch of RADARSAT-2, TerraSAR-X, COSMO SkyMed and SENTINEL-1 brought new imaging modes and high resolution data on regular basis for the ocean monitoring [4].

Earlier the ENVISAT data was mostly used for the operational oil spill detection till the end of the mission in 2012. Afterwards its place have been taken by the SENTINEL-1A mission launched in April 2014 and 1B launched in April 2016. There is a lot of information about the SENTINEL missions on the ESA official website [40].

The two SENTINEL-1 satellites are identically constructed and have near-polar, sun-synchronous orbit with 12 days repeat cycle for each satellite, making a 6-day revisit time for the European land and sea area. They share the same orbit plane with 180° orbital phasing difference. The satellites use HH–HV or HH polarization for monitoring the polar and sea-ice areas and VV–VH or VV polarization for the other land and water observations. The planning of European Space Agency is to launch SENTINEL-1C and SENTINEL-1D in 2021 and 2023 respectively.

The SENTINEL-1 mission has a single C-band synthetic aperture radar instrument working at a central frequency of 5.405 GHz and programmable bandwidth of 0–100MHz. It operates in four exclusive acquisition modes – Stripmap (SM – used only on request for extraordinary events), Interferometric Wide swath (IW – main operational mode for most service requirements), Extra-Wide swath (EW) and Wave mode (WV). Table 1 summarizes the important information for the SENTINEL-1 acquisition modes and figure 3 pictures the SENTINEL-1 product modes visually.

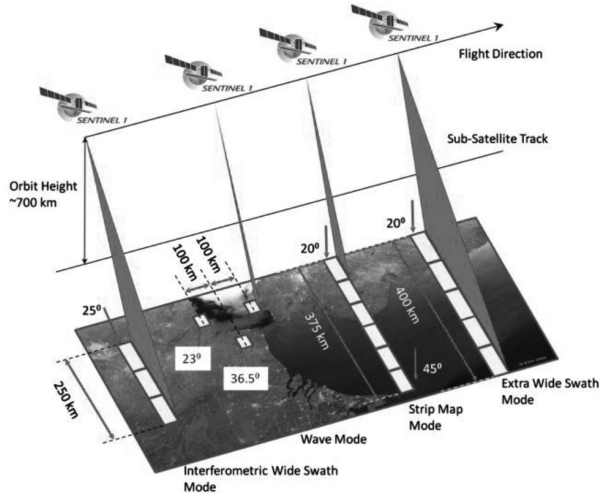


Fig. 3. Operation modes for SENTINEL-1A and B satellites, from [40]

Table 1. Operation modes of the SENTINEL 1 satellite mission, from [40]

Mode	Incidence Angle [deg]	Resolution [m]	Swath Width [km]	Polarization
Stripmap	20–45	5×5	80	HH+HV, VH+VV, HH, VV
Interferometric Wide swath	29–46	5×20	250	HH+HV, VH+VV, HH, VV
Extra Wide swath	19–47	20×40	400	HH+HV, VH+VV, HH, VV
Wave	22–35 35–38	5×5	20×20	HH, VV

The SENTINEL missions are of a particular interest for the research community due to the free access to the data base. The website of the Copernicus Open Access Hub [41] provides data from the SENTINEL-1, 2 and 3 missions freely after a short registration. Satellite images gained on different bands, with great accuracy and spatial resolution are provided on weekly basis, opening new opportunities for non-commercial research.

The TerraSAR-X mission is a German satellite mission launched by DLR in June 2007 with scientific and commercial purposes. Its lifespan was planned for 5 years, but more than 10 years after the launch, it is still operational. The high resolution images of the mission are used for hydrology, geology, climatology, oceanography, cartography, environmental and disaster monitoring. The SAR antenna in flight attitude points at 33.8° off nadir. It runs on a sun-synchronous circular down-dusk orbit with a revisit period of 11 days. It is equipped with a

X-band SAR antenna with 31 mm wavelength or a 9.6 GHz frequency. The spatial resolution is 40 m and the coverage is up to 270×200 km² making it suitable for observation of even small oil spills. It is also particularly useful for ship detection.

TanDEM-X is the follow-up twin mission of TerraSar-X, launched 3 years later, in June 2010. It has a high vertical accuracy better than two meters and together with TerraSAR-X it is from the first configurable synthetic aperture radar interferometers. TanDEM-X flies in close formation to TerraSAR, only couple of hundred meters apart, monitoring the Earth from different angles. More information about the missions can be found on the official DLR-website [42].

The satellite RADARSAT-2 was launched by the Canadian Space Agency in December 2007 and is still actively monitoring the Earth. It is a commercial mission, enhancing marine surveillance, ice monitoring, disaster management, environmental monitoring, resource management and mapping. RADARSAT-2 is equipped with a C-Band active antenna with centre frequency of 5.405 GHz and bandwidth of 100 MHz. On the website of CSA there is some more valuable information about the mission [43].

4. ALGORITHMS

With the growing amount of satellite data over different ocean and sea regions worldwide the possibilities for marine monitoring have increased dramatically. The manual image processing is time consuming and requires the availability of skilled operators which is significant limitation for the process optimization. Considering that a fast reaction is crucial for undertaking adequate counteractions, the importance of an automatized process for oil spill detection arises.

For the automatic detection of anomaly sea patterns, or dark objects as they appear on SAR images, there are certain procedures during the image processing which should be done in order to detect spills.

The first step when working with raw SAR data is always the pre-processing of the image. This includes image calibration, land masking and speckle reduction. These steps enhance the visibility of dark areas and make the distinction of their borders easier. Secondly, the dark spots are detected and isolated in a segmentation process. There are different techniques however mostly this is done using thresholding. In the third part of the detection algorithm a set of features is extracted and calculated for the detected dark objects. The classification process is the last step and it strongly depends on the information gained by the previous two steps. An extensive archive of correctly classified dark objects for training the algorithms and information about the local meteorological conditions is a helpful contribution for distinguishing between actual oil spills and look-alikes.

The image segmentation and feature extraction are the most important steps for the automatic oil spill detection. If here a dark area is not detected or the features lead to misleading conclusions an oil spill can remain undetected.

The dark formation identification is the first crucial step in oil spill detection. For the automatic approach a threshold algorithm, adaptive or not, can be applied. An early attempt of this technique is presented in [44], where the bimodal histograms in a set window is analysed. It was proven as a good procedure for thick spills; however the thin spills remain undetected. A similar approach was presented in [45], where a comparison between bimodal histogram method and adaptive thresholding is presented. Later it was shown that bimodal histogram provides decent results [46]. This algorithm was firstly developed for RADARSAT-1 SAR data and it spatially averages the image before applying an adaptive thresholding.

Simple thresholding algorithms use one value for the whole image and all pixels are compared to it. This value is usually one half of the average Normalized Radar Cross Section (NRCS) of the image or NRCS minus the standard deviation [47].

The adaptive thresholding uses a threshold value, which is calculated locally for areas covered by a moving window. Solberg et al. [48, 49] uses a threshold value of k dB below the mean value of the moving window. The value of k is calculated using a multi-scale pyramid approach and a clustering step. Karathanassi et al. [50] uses a fully adaptive value to local contrast variations. The technique of hysteresis thresholding was firstly described by [51]. It detects the edges of Gaussian-smoothed image and linear dark formations are successfully detected [52].

Another method based on the Laplace of Gaussian (LoG) and Difference of Gaussian (DoG) operators are presented in [53]. Firstly the original image is reduced by a unit of 2 by 2 pixels and multilayer images with decreased effect of noise and sea clutter are created. For the detection of dark areas the LoG derivative operator is applied. The sharpness of the oil spill shape is measured with a first order derivative operator – DoG. This effect is notable because water and oil are electromagnetically different. This makes the gradient of the image grey value on the water-oil boundary different. The wavelet packet transformation is a segmentation technique proposed by Liu et al. [54] and its linear feature detection scheme with LoG-operator as analysing wavelet. It is analogous to Fourier transformations, but localized in frequency and time. For the transformation are selected areas with multiple histogram peaks and for the extraction of small scale features is taken an edge detector wavelet transformation [54, 55]. The 2D wavelet transformation is highly efficient bandpass filter and can separate various scale processes delivering phase/location information in SAR image. It is good for near real-time screening of satellite data, data reduction and image enhancement.

The fuzzy clustering is a method where for each pixel a function is selected, which measures how much the pixel belongs to a certain value. Afterwards the Fuzzy C means (FCM) algorithm is applied and a pyramid structure is used to

find membership values. The uncertain pixels are arranged in the lower pyramid level. A Sobel operator is used to enhance main edges of the original filtered image [56]. Firstly a fuzzy clustering is taken for preliminary partition of the pixels on the basis of grey level intensities and then simple cluster validity criterion is done to determine the optimal number of clusters present in the data. Another method for dark object segmentation is based on using mathematical morphology for the image segmentation [57]. The aim is to detect spills from moving tankers which is implemented in the selected features (elongatedness and spill dampening). An advantage of this method is that there is no need for prior knowledge about ocean conditions and it is also good for features extraction used in the decision process.

5. FEATURES

The different methods described in the previous part are used for the detection of suspicious structures on sea surface. Hereby it is important that during the detection algorithm the shape of the object is preserved as it is the one of the keys for distinguishing between actual oil slicks and look-alikes.

For creating a working oil spill detection algorithm the dark objects should be characterized following a certain characterization criteria. Every algorithm has a different set of features, but generally they can be organized in four classes.

The spatial geometry and shape of the dark object is analysed in almost every oil spill detection algorithm. Considering this information together with of some regional specifications of winds and currents, the differentiation between oil slicks and other surface patterns might be enhanced. Very often oil is discharged from moving tankers. In that case calculating the elongatedness, or the ratio between width and length of the dark object, is a very useful feature [57].

The backscattering level of the dark object and the surrounding is another informational class of features. For a neural networks classification backscattering ratios of different regions are considered as crucial [58]. The backscattering of the background surrounding is important due to wind speed dependence as well [47].

In the set of features the contextual positioning of the dark object is of particular interest. An additional database containing the locations of oil pipelines, platforms or the vessel traffic information might contribute significantly to the correct classification. Wind history is also useful for slick classification and age estimation [59].

The texture of a SAR image provides information about the spatial correlation between neighbouring pixels. The comparison between pixels of different regions on the SAR image puts the dark object in correlation with other regions.

In the following paragraphs the set of features for three different algorithms – adaptive thresholding, statistical classification method and neural networking – are observed.

Solberg et al. [60] has analysed Radarsat and ENVISAT SAR images with an adaptive thresholding algorithm. The observed features are:

- Slick complexity
- Slick power-to-mean ratio
- Slick local contrast
- Slick width
- Slick local neighbours
- Slick global neighbours
- Border gradient
- Slick area
- Distance to detected ship
- Slick planar moment
- Number of regions in the image
- Slick smoothness contrast

Fiscella et al. [47] describes an oil spill detection method where low resolution images are inspected for the presence of suspicious structures manually or automatically. Later the detected dark formations are classified using a Mahalanobis classifier and a compound probability classifier – both statistical classification methods.

For the automatic analysis of a SAR image the dark areas with Normalized Radar Cross-Section (NRCS) lower than one half of the average NRCS of sea area are selected. The actual oil spill detection is done after identification of the border of the dark object and evaluation of the following direct features:

- Perimeter
- Area
- Average NRCS inside the dark area
- Average NRCS in a limited area outside the dark area
- NRCS dark area standard deviation
- NRCS outside dark area standard deviation
- Gradient of the NRCS across the dark area perimeter
- Form factor: the dispersion of dark area pixels from its longitudinal axis.

Afterwards from this set of features the following quantities are derived/calculated:

- Perimeter to area ratio
- Intensity ratio between average NRCS inside and outside the dark area
- NRCS standard deviations ratio inside and outside the dark area
- Ratio between NRCS intensity and its standard deviation inside the dark area
- Ratio between NRCS intensity and its standard deviation outside the dark area
- The ratio of the last two ratios.

Then the classification procedure is undertaken.

In Del Frate et al. [58] a neural network algorithm is used for the dark object classification. A long time series of over 600 images from the years 1997 and 1998 over different areas in the Mediterranean Sea is analysed. A histogram for every image is generated and the borders of the dark object are determined. The features needed for the dark object classification are the following:

- Area of the object A
- Perimeter P
- Complexity C defined as $C = \frac{P}{2\sqrt{\pi A}}$
- Spreading S – low value for long and thin objects and high for objects closer to circular shape
- Object standard deviation
- Background standard deviation
- Max contrast – difference between background mean value and the lowest value inside the object
- Mean contrast
- Max gradient
- Mean gradient
- Gradient standard deviation.

6. CLASSIFICATION METHODS

The last step of the oil slick detection is the classification procedure, undertaken in order to distinguish the actual oil slicks from look-alikes (for example anomaly alga blooms, sewage water discharges, surface water currents or capillary wave damping caused by local winds).

There are several classification methods published in the literature. An easy and common way for dark object classification is the use of statistical classifiers, where the decision is based on probability calculations. They are simple and reliable and the output can be easily reproduced.

Fiscella et al. [47] is testing a Mahalanobis [61] and a compound probability classifier where the probability of a dark object being an oil slick is calculated. The Mahalanobis classifier is comparing the set of characteristic features (written in the input vector \mathbf{x}) with a template, composed from previous measurements. For this technique the Mahalanobis distances between the calculated set and the class's oil spill m_1 or look-alike m_2 is computed. The Mahalanobis distance r_j^2 is given by

$$r_j^2 = (\mathbf{x} - m_j)'C^{-1}(\mathbf{x} - m_j)$$

in the matrix form with $j = 1,2$ and C the covariant matrix of x . For the classic compound method the probability p for a dark object being an oil spill is calculated using

$$p = \frac{1}{1 + \prod q_i(x_i)/p_i(x_i)},$$

where $p_i(x_i)$ are the probability distribution functions for oil spill and $q_i(x_i)$ for look-alike classes.

A data set of 123 images was tested [47] and the correctly classified data with the Mahalanobis classifier for $p_{\text{Mah}} > 2/3$ is 78% and for $p_{\text{Mah}} > 1/2$ is 83%. The compound probability classifier delivers correctly classified data with $p_{\text{Com}} > 2/3$ is 79%, and $p_{\text{Com}} > 1/2$ is 82%.

A similar method based on statistical modelling with a rule based approach is using the Gaussian density function and is presented by Solberg et al. [48]. Similar to Fiscella et al. [47] a template set is used, but here it is derived from a signature database of 7.051 dark objects containing 71 oil spills and 6.980 look-alikes. The method classified correctly 94% of the oil spills and 99% of the look-alikes.

Another widely used method is the neural network classifier. It is considered effective because it operates well with nonlinear mapping of multidimensional input on single-dimensional output and complex statistics. Different from other statistics based classifier; the neural network approach doesn't need well defined relationship between input and output vectors, as it determines it after analysing a set of training data.

The neural network algorithm is a mathematical tool for calculating the probability of occurrence of a certain event. This is done by creating an input term which is then mathematically manipulated through multiple neurons where each calculates the sum of the inputs adds a bias term and then provides the result to the up-following neurons. The model topology is specific for each neural network and gives how the input, output and the hidden units are interconnected. In the feedforward network, which is also applied for the oil spill case, the input flows only forward to the next-level neurons and cannot return to the previous layers.

Del Frate et al. [58] used in their extensive study a neural network classification algorithm. They analysed 600 ERS images from which they extracted 139 images with dark objects, 71 of which were oil spills and 68 – look-alikes. More details about the exact functioning principles can be found in the publication. Before analysing the actual images the system is trained in order to get optimized results for the given issue. Once trained the network has examined the given pictures. It has misclassified 18% of real oil spills on the images as look-alikes and 10% of the look-alikes were wrongly classified as oil. The overall rate of misclassified pixels is 14%.

A more recent study based on article neural network is presented in [62] with 91.6% correctly classified oil spills and 98.3% look-alikes.

Another classification method based on fuzzy classification rules is presented by Karathanassi et al. [50]. Firstly homogeneous dark objects are extracted in any given resolution using a threshold technique, adaptive to any local contrast and

later they are classified using a fuzzy logic. Each feature of the calculated set is considered as a separate class and each class consists of a set of fuzzy expressions. This makes the logical operation and the estimation of each specific value more accurate. The method processed 12 SAR images and classified successfully high percentage of the oil spills and the look-alikes.

It is difficult to compare the skill of the different classification methods, because they use different data sets, the dark object algorithms function differently and the set of features vary. Therefore the reported classification accuracy cannot be compared directly.

Analogously it is hard to compare the computational time and make statements which technique delivers fastest the most accurate results. Analysing the same data set using different segmentation techniques, features and classification methods could deliver valuable information for possible advantages and disadvantages.

7. EXAMPLES

Regional studies focusing on the local specifications of the different water basins have been done for most of the European seas. Several initiatives exist, monitoring European waters and delivering real-time information about oil spills. This is very important considering that a fast reaction is crucial for identifying the polluter.

The platform Oceanides [63] is a database with information collected from observations via aircraft and satellite radar images, all available from a single source. The project is funded by the European Commission as part of CORDIS (Community Research and Development Information Service). Oceanides is focused on marine monitoring and can be used for different purposes. The tool organizes the data depending on the interest of the operator and assembles the knowledge required to establish a more effective monitoring of oil pollution and identification of possible polluters. It is operational for European waters and is already implemented on regional scale for oil pollution monitoring.

Another on-line platform created for oil spill detection is CleanSeaNet [64]. This platform is a project of the European Maritime Safety Agency which is a decentralized EU agency. CleanSeaNet is a service focused on identification of oil spills, combined with vessel detection in European waters and it works by analysing radar satellite images. The images are processed within 30 minutes after the satellite passes overhead and an alarm for potential pollution is issued directly after. Correlating satellite data of detected vessels with vessel traffic reports increases the possibility of correctly identifying the polluter.

CleanSeaNet collects supplementary data such as optical marine images and oceanographic and meteorological information, which significantly increases the correct detection ratio.

For Bulgaria the Black sea is of a particular interest considering the geographical location and the importance to the region.

The extensive study of Malinovsky et al. [65] deals with the SAR analysis for oil spill detection particularly for the Black sea region. Using the polarization ratio in the ENVISAT Alternating Polarization Images they have detected 424 oil spill events in proximity to the major ship routes and oil platforms.

Ivanov and Kucheiko [66] have studied SAR images of the Eastern Black sea (2011–2013) and the Northern & Middle Caspian Sea (2009–2013) and compared the extend and source of the oil pollutions, finding very different results for the both regions. The oil spills in the Black sea are caused mainly by ships (tank washings and deliberate illegal discharges) and have a great extend up to 320 km². Those in the Caspian sea are of a much smaller surface area not exceeding 70 km² coverage [66].

Other studies of oil-spills in the Black sea are presented by [67–69], where different observation methods for oil slicks detection are applied.

In the past there were attempts to establish a real time monitoring system for tracking oil spills in Black sea as well; however as to the present moment they are not operational.

The online platform of JRC (Joint Research Centre) published information on the oil-spills discovered in the Black Sea in the period 2000–2004 (<http://publications.jrc.ec.europa.eu/repository/handle/JRC55159>).

The results were used in the project of the Commission on the Protection of the Black Sea Against Pollution (http://www.blacksea-commission.org/_projects_MONINFO.asp) "Monitoring and Information Systems for Reducing Oil Pollution" implemented in the period 2009–2010 with the main objective to prevent and take measures against operational/accidental/illegal oil pollution.

8. CONCLUSIONS

Spaceborne SAR sensors have proven to be most efficient among others for oil spill detection and their capacity for long-term, large-scale ocean monitoring has been demonstrated. Their good spatial resolution and feasibility at all-weather, all-time makes them a reliable source for long time series data. The latter is determining for creating a fully automatized method for oil spill detection, since every algorithm needs a data base for training, so that the dark object classification can be performed with a minimum false alarm ratio.

In this article various algorithms for oil spill detection have been presented, all of which deliver reasonable results. It is important to stress the fact that their success ratio cannot be compared directly, since all use different data sets with different quality. Moreover a serious limitation is the use of unverified data. For the determination of the success ratio the dark objects should be classified as oil spill or

look-alike, based on the optical inspection of the SAR images, done by an operator, which is not always an available approach.

It is not trivial to apply a working detection algorithm to a new sea area. In order to create an operational procedure for a particular geographic region some specifications of the water basin should be considered. Those include local topography, water density, colour, seasonal variations in alga blooms, winds and currents and the coastal borders.

In general, creating a fully automatized detection method is a challenging task, considering the long list of limitations. A semi-automatic method might be more beneficial considering the success ratio.

In this review different methods for the image segmentation procedure for extraction of dark objects are presented – adaptive and hysteresis thresholding algorithms, a method using the Laplace of Gaussian and Difference of Gaussian operators, a wavelet packet transformation, fuzzy clustering method and one, based on mathematical morphology.

For the correct classification of dark formations the extraction and computation of a set of features, different for every algorithm, is crucial. The major feature classes are presented together with some concrete examples.

Different classification procedures are presented – one based on probability methods, another using the Gaussian density function, a neural network algorithm and a fuzzy classifier. The success ratios for the different approaches are listed.

REFERENCES

- [1] Antonucci, R. *ARA& A*, 1993, **31**, 473.
- [2] Antonucci, R., J.S. Miller. *ApJ*, 1985, **297**, 621.
- [3] Tran, H. D. *ApJ*, 2001, **554**, L19.
- [4] Tran, H. D. *ApJ*, 2003, **583**, 632.
- [5] Lumsden, S. L., D. M. Alexander. *MNRAS*, 2001, **328**, L32.
- [6] Shu, X.W., J.X. Wang, P. Jiang, et al. *ApJ*, 2007, **657**, 167.
- [7] Nicastro, F., A. Martocchia, G. Matt. *ApJ*, 2003, **589**, L13.
- [8] Petrov, G. P., I. M. Yankulova. *NewA*, 2012, **17**, 137.
- [9] Marinucci, A., S. Bianchi, F. Nicastro, et al. *ApJ*, 2012, **748**, 130.
- [10] Ho, L. C., J. E. Greene, A.V. Filippenko, et al. *ApJS*, 2009, **183**, 1.
- [11] Tremaine, S., K. Gebhardt, R. Bender. *ApJ*, 2002, **574**, 740.
- [12] Ho, L. C., A.V. Filippenko, W. L.W. Sargent. *ApJS*, 1997, **112**, 315.
- [13] Panessa, F., L. Bassani. *A&A*, 2002, **394**, 435.
- [14] Panessa, F., L. Bassani, M. Cappi, et al. *A&A*, 2006, **455**, 173.
- [15] Bianchi, S., A. Corral, F. Panessa, et al. *MNRAS*, 2008, **385**, 195.
- [16] Bassani, L., M. Dadina. *ApJS*, 1999, **121**, 473.
- [17] Lamastra, A., S. Bianchi, G. Matt, et al. *A&A*, 2009, **504**, 73.
- [18] Moran, E. C., A. J. Barth, L. E. Kay, et al. *ApJ*, 2000, **540**, L73.
- [19] González-Martín, O., J. Masegosa, I. Márquez, et al. *ApJ*, 2009, **704**, 1570.
- [20] Vasudevan, R. V., A. C. Fabian. *MNRAS*, 2009, **392**, 1124.